J. Astrophys. Astr. (2001) **22**, 51–80

Carbon Recombination Lines from the Galactic Plane at 34.5 & 328 MHz

N. G. Kantharia[1]* & K. R. Anantharamaiah [2]†
[1]*National Centre for Radio Astrophysics (TIFR), Pune 411007, India*
[2]*Raman Research Institute, Bangalore 560080, India*

Received 2000 September 14; accepted 2000 November 25.

Abstract. We present the results of a search for carbon recombination lines in the Galaxy at 34.5 MHz (C575α) made using the dipole array at Gauribidanur near Bangalore. Observations made towards 32 directions resulted in detections of lines in absorption at nine positions. Followup observations at 328 MHz (C272α) using the Ooty Radio Telescope detected these lines in emission. A VLA D-array observation of one of the positions at 330 MHz yielded no detection implying a lower limit of 10′ for the angular size of the line forming region.

The longitude-velocity distribution of the observed carbon lines indicate that the line forming regions are located mainly between 4 kpc and 7 kpc from the Galactic centre. Combining our results with published carbon recombination line data near 76 MHz (Erickson, McConnell & Anantharamaiah 1995), we obtain constraintson the physical parameters of the line forming regions. We find thatif the angular size of the line forming regions is $\geq 4°$, then the range of parameters that fit the data are: $T_e = 20 - 40$ K, $n_e \sim 0.1 - 0.3$ cm^{-3}and pathlengths $\sim 0.07 - 0.9$ pc which may correspond to thin photo-dissociated regions around molecular clouds. On the other hand, if the line forming regions are $\sim 2°$ in extent, then warmer gas ($T_e \sim 60 - 300$ K) with lower electron densities ($n_e \sim 0.03 - 0.05$ cm^{-3}) extending over several tens of parsecs along the line of sight and possibly associated with atomic H I gas can fit the data. Based on the range of derived parameters, we suggest that the carbon line regions are most likely associated with photo-dissociation regions.

Key words: Interstellar medium: clouds, lines, line profiles, radio lines.

*e-mail: ngk@ncra.tifr.res.in
†e-mail: anantha@rri.res.in

1. Introduction

Radio recombination lines have been extensively used to investigate the ionized component of the interstellar medium. Recombination lines of hydrogen, helium and carbon have been unambiguously identified in the spectra obtained towards H II regions. Since the ionization potentials of hydrogen (13.6 eV) and helium (24.4 eV) are relatively high, these elements are ionized by the strong UV radiation in the vicinity of O and B stars. Therefore radio recombination lines of H & He generally trace hot ionized regions ($T_e \sim$ 5000–10000 K). On the other hand, the first and second ionization potential of the fourth most abundant element, carbon are 11.4 eV and $\sim$ 24 eV. Carbon is likely to be doubly-ionized inside the H II regions. However, lower energy photons (E $<$ 13.6 eV) which escape from the H II regions can singly-ionize carbon both in the immediate vicinity of the H II region (if the H II region is ionization bounded) as well as in the interstellar clouds which may be farther away. In these regions where hydrogen, helium and oxygen are largely neutral and where carbon and few other elements with lower ionization potential (e.g. sulphur) are singly ionized, the temperatures are likely to be much lower i.e. less than a few hundred K. Radio recombination lines of singly-ionized carbon, thus, generally trace cooler regions of the interstellar medium.

The C II regions detectable in recombination lines can be categorized into two types. The first type are the ionized-carbon regions which occur in the immediate vicinity of some bright H II regions such as W3 and NGC 2024. We shall refer to such regions as classical C II regions since these are carbon Stromgren spheres around a central star. Carbon recombination lines were first detected from such classical C II regions by Palmer *et al.*(1967) at a frequency of $\sim$ 5 GHz and have subsequently been studied at $\nu >$ 1 GHz towards many H II regions using both single dishes and interferometers (e.g. Pankonin *et al.*1977, van Gorkom *et al.*1980, Roelfsema *et al.*1987, Onello & Phillips 1995, Kantharia *et al.*1998a). Carbon recombination lines from classical C II regions are narrow ($4 - 10$ kms^{-1}) and are sometimes comparable in strength to the hydrogen recombination line observed from the associated hot H II region. Both the narrow width and intensity of the line suggest that the carbon line originates in a cooler ($<$ few hundred K) region where stimulated emission of the background continuum is likely to cause enhanced line emission. Classical C II regions are generally observed in carbon recombination lines at frequencies $\nu \geq$ 1 GHz. To our knowledge no carbon recombination line from classical C II regions has been detected below 1 GHz.

A second class of C II regions, which we will refer to as diffuse C II regions, and which this paper is mainly concerned with, were discovered by Konovalenko & Sodin (1980). Using the UTR-2 low-frequency radio telescope in Ukraine, Konovalenko & Sodin (1980) observed an absorption line at 26.13 MHz in the direction of the strong radio source Cas A. This low-frequency absorption feature was later correctly identified by Blake, Crutcher & Watson (1980) as the C631α recombination line arising in a region at a temperature of $\sim$ 50 K and electron density $\sim$ 0.1 cm^{-3}. The region was tentatively identified with the diffuse neutral H I clouds in

the Perseus arm. Since then, the direction of Cas A has been observed in recombination lines of carbon at frequencies ranging from 14 MHz to 1420 MHz (Payne *et al.*1989, Payne *et al.*1994 and the references therein). The most recent results (Kantharia *et al.*1998b) suggest that the diffuse C II region in the Perseus arm towards Cas A could be at a temperature of ~75 K with an electron density of ~0.02 cm^{-3}, which supports the identification of these regions with neutral H I clouds. Interferometric observations of the spatial distribution of the C272α carbon line (near 332 MHz) over the face of Cas A also supports this association (Anantharamaiah *et al.*1994, Kantharia *et al.*1998b). The low-frequency recombination lines from diffuse C II region towards Cas A exhibit interesting characteristics. The lines which are in absorption below 150 MHz turnover into emission above 200 MHz. Moreover, the width of the lines increase dramatically towards lower frequencies because of pressure and radiation broadening. The variation of line strength and line width with frequency are important diagnostics of the physical conditions in the line forming regions.

If the diffuse C II regions which are detected in low-frequency recombination lines of carbon towards Cas A are associated with the neutral H I component of the interstellar medium, then it may be expected that such low-frequency lines are a widespread phenomenon. Detections have indeed been made in several other directions. Carbon recombination lines were detected in absorption near 25 MHz from the directions of G75.0+0.0 & NGC 2024 by Konovalenko (1984a) and towards L1407, DR21 & S140 by Golynkin & Konovalenko (1991). Anantharamaiah *et al.*(1988) detected absorption lines near 75 MHz towards M16 and the Galactic Center. With hindsight, it now appears that the carbon lines detected in emission near 327 MHz using the Ooty Radio Telescope towards 14 directions in the galactic plane by Anantharamaiah (1985) belong to this category. The first major fruitful search for low-frequency recombination lines of carbon was conducted by Erickson *et al.*(1995) at 76 MHz using the Parkes radio telescope in Australia. Absorption lines of carbon were detected from all the observed positions with longitudes $< 20^\circ$ in the Galactic plane. These observations showed that diffuse C II regions are a common phenomenon in the inner Galaxy.

In this paper, we present observations of recombination lines of carbon around 34.5 MHz made using the low-frequency dipole array at Gauribidanur (which is near Bangalore, India) and around 328 MHz made using the Ooty Radio Telescope (ORT). Out of the 32 directions, most of them in the galactic plane, that were searched at 34.5 MHz, lines were detected in absorption towards nine directions. At 327 MHz, twelve positions were observed and lines were detected in emission towards seven of these. Six of the detected lines are common to 34.5 MHz and 328 MHz. To obtain an estimate of the size of the line-forming region, observations were made with two angular resolutions ($\sim 2^\circ \times 2^\circ$ and $\sim 2^\circ \times 6'$) using the ORT. We also followed up one of the detections with observations near 332 MHz using the D-Configuration of the Very Large Array. All the six directions towards which lines were detected here at 34.5 MHz and 328 MHz, have also been detected at 76

MHz by Erickson *et al.*(1995). In this paper, we combine the results at these three frequencies to constrain the nature of the line forming region.

This paper is organized as follows. In Section 2, the observations at 34.5 MHz using the Gauribidanur dipole array, at 327 MHz using the Ooty Radio Telescope and at 332 MHz using the Very Large Array are described and the results are presented. In Section 3, we obtain constraints on the sizes of the line forming regions using line ratios observed with different angular resolutions. The probable location of the line forming region in the galactic disk is constrained using an $l - v$ diagram of the observed lines. In Section 3, we also derive constraints on the combination of electron density, temperature and radiation field surrounding the line forming region using the variation of line width with frequency. Section 4 is devoted to modelling the line forming region by fitting the observed variation of integrated optical depth with frequency. In Section 5, the results of modelling are discussed in the light of what we know about the interstellar medium. Finally the paper is summarized in Section 6.

2. Observations and Results

2.1 *Gauribidanur observations near 34.5 MHz*

The low-frequency dipole array at Gauribidanur which operates near 34.5 MHz (Deshpande *et al.*1989 and references therein) was used during July–October 1995 to observe several α–transitions (Δn = 1) with principal quantum numbers ranging from n = 570 to 580. The Gauribidanur radio telescope is a meridian transit instrument consisting of 1000 broadband dipoles arranged in a T-shaped configuration. The East-West (EW) arm consists of 640 dipoles, distributed over a distance of 1.38km whereas the North-South arm extends southwards from the centre of the EW arm and consists of 360 dipoles laid over a distance of 0.45 km. The present set of observations were carried out using the EW arm in total power mode, which gave an angular resolution of $\sim 21' \times 25°$ ($\alpha \times \delta$) at zenith. The effective collecting area of the EW arm is $160\lambda^2$ (λ=8.67 m).

The Gauribidanur telescope has limited tracking facility (Deshpande *et al.*1989) which enables the array to track a source with declination δ, for a period of 40secδ minutes about its transit time. Since these low-frequency recombination lines are weak, each position would have required several weeks of observations with the Gauribidanur telescope to reach the desired sensitivity. In order to reduce the total duration of the observations, we employed a multi-line receiver in which eight different transitions with $\Delta n = 1$ near $n = 575$ were observed simultaneously and the spectra averaged. The details of the multi-line receiver and the observing procedure have been described in Kantharia *et al.*(1998b).

The data collected were carefully examined and all those affected by interference were removed. The final spectrum was obtained by averaging all the observed transitions. The spectra are hanning smoothed and therefore have a resolution of 0.5 kHz. The total bandwidth is 32 kHz ($\sim$ 250 kms^{-1}).

Table 1. List of sources that were searched for carbon radio recombination lines at 34.5 MHz.

Position	$\alpha(1950)$	$\delta(1950)$	Central Vel setting	$\frac{\Delta T_{rms}}{T_{sys}}$	Effective int time
	hh mm ss	° ′ ″	kms^{-1}	$\times 10^{-3}$	hours
G342+00	16 50 34	-43 37 38	-20.0	0.35	63.5
G352+00	17 21 47	-35 37 25	-20.0	0.20	95.3
G00+00	17 42 27	-28 55 00	0.0	0.20	58.7
G05+00	17 54 00	-24 37 59	0.0	0.23	70.3
G10+00	18 04 47	-20 17 51	0.0	0.20	91.3
G14+00	18 12 59	-16 48 00	20.0	0.22	55.0
G16.5+00	18 17 57	-14 36 18	25.0	0.22	68.3
G25+00	18 34 12	-7 05 51	45.0	0.23	78.3
G45.2+00	19 11 44	10 48 50	20.0	0.23	45.8
G50+00	19 21 02	15 02 41	25.0	0.27	108.0
G55+00	19 31 08	19 25 32	25.0	0.23	50.7
G63+00	19 48 31	26 21 12	20.0	0.19	72.0
G75+00	20 19 02	36 26 46	0.0	0.15	188.0
G81+00	20 37 17	41 16 58	25.0	0.31	114.0
G85+00	20 23 08	21 22 05	25.0	0.34	41.7
G97+00	21 42 21	52 56 10	-20.0	0.29	91.5
G99+00	21 52 47	54 11 59	-20.0	0.33	169.5
G100+00	21 58 15	54 48 34	-20.0	0.20	178.3
G125+00	01 06 22	62 31 58	-20.0	0.37	88.8
G130+00	01 48 45	61 47 14	-20.0	0.37	128.5
G145+00	03 34 08	55 24 12	-20.0	0.37	100.0
S 140	22 17 36	63 04 00	-20.0	0.39	24.3
DR 21	20 37 13	42 09 00	0.0	0.35	28.3
Orion	05 32 48	-05 27 00	0.0	0.54	19.7
Cygnus Loop	20 49 30	29 50 00	25.0	0.16	99.8
Cygnus A	19 57 45	40 36 00	0.0	0.23	62.3
W3	02 21 50	61 53 20	-50.0	0.39	238.8
W49	19 08 51	09 02 27	60.0	0.46	42.9
W51	19 20 17	14 02 01	50.0	0.20	69.0
G203.1+2.1	06 38 17	09 43 20	8.0	0.5	12.0
G224.6-2.4	07 01 56	-11 23 55	15.0	0.22	49.1
Rosette Nebula	06 29 18	04 57 00	0.0	0.34	37.5

We observed 32 positions, most of these being in the Galactic plane. Table 1 gives the observational parameters. The observable positions were limited by the transit nature of the Gauribidanur telescope. Within the declination range accessible to the Gauribidanur telescope ($-45°$ to $75°$), the selection of positions was determined partly by the strong Galactic background in the inner Galaxy and partly by the positive results of other low-frequency observations (Konovalenko 1984a, Anantharamaiah 1985, Golynkin & Konovalenko 1991). Carbon recombination lines were detected in absorption from nine of these directions. At such high quantum levels, collisions thermalize the level populations and since the brightness temperature of the non-thermal background radiation field is much higher than the temperature of the thermal gas, the lines appear in absorption. The spectra obtained towards nine of the directions are shown in Fig. 1. The results from a high signal-to-noise ratio spectrum obtained towards Cas A have been presented in a separate publication (Kantharia *et al.*1998b). The peak line-to-continuum ratios observed towards the nine directions shown in Fig. 1 are of the order of a few times 10^{-4}. Gaussians were fitted to the detected spectra and the parameters are listed in Table 2. No lines were detected from the other positions to a 5σ limit of 5.0×10^{-4}. In almost all the cases, only a linear baseline had to be removed to obtain the final spectra.

A relatively strong absorption line of carbon was detected from the direction of the Galactic centre (G00 + 00) as shown in Fig. 1. Carbon recombination lines have been observed from this direction in absorption at 76 MHz (Anantharamaiah *et al.*1988, Erickson *et al.*1995), 42 MHz (Smirnov *et al.*1996) and in emission at 408 MHz (Pedlar *et al.*1978) and 328 MHz (Anantharamaiah 1985, Roshi & Anantharamaiah 1997).

Carbon lines were detected from all the six observed directions in the inner galactic plane ($l = 352° - 17°$). This result is similar to that of Erickson *et al.*(1995) who detected carbon recombination lines near 76 MHz from all their observed positions in the longitude range 342° to 20°. We also detected lines near 34.5 MHz from DR 21, G63+00 and G75+00. The lines detected are either at positive velocities or close to 0 kms^{-1} . The line-to-continuum ratios of these lines range from a few times 10^{-4} to 10^{-3} and the width-integrated line-to-continuum ratio ranges from 1.5 to 4 s^{-1}. The lines have widely varying widths with the narrowest lines ($\sim$ 19 kms^{-1}) occurring towards DR 21 and the broadest lines ($\sim$ 54 kms^{-1}) towards G14+00. Erickson *et al.*(1995) have also observed line widths (near 76 MHz) ranging from 5 kms^{-1} to 47 kms^{-1} .

The carbon line observed towards G10+00 appears to be composed of two components. Parameters derived from a double component Gaussian fit to this profile are listed in Table 2. A similar trend is also seen in the profiles towards G05+00 and G14+00. However, the signal-to-noise is not adequate for a double component fit.

The rms noise and the effective integration time on the spectra with no detection are listed in Table 1. The spectra were smoothed to a spectral resolution corresponding to a typical line width ($\sim$ 20 kms^{-1}) and the spectra were again

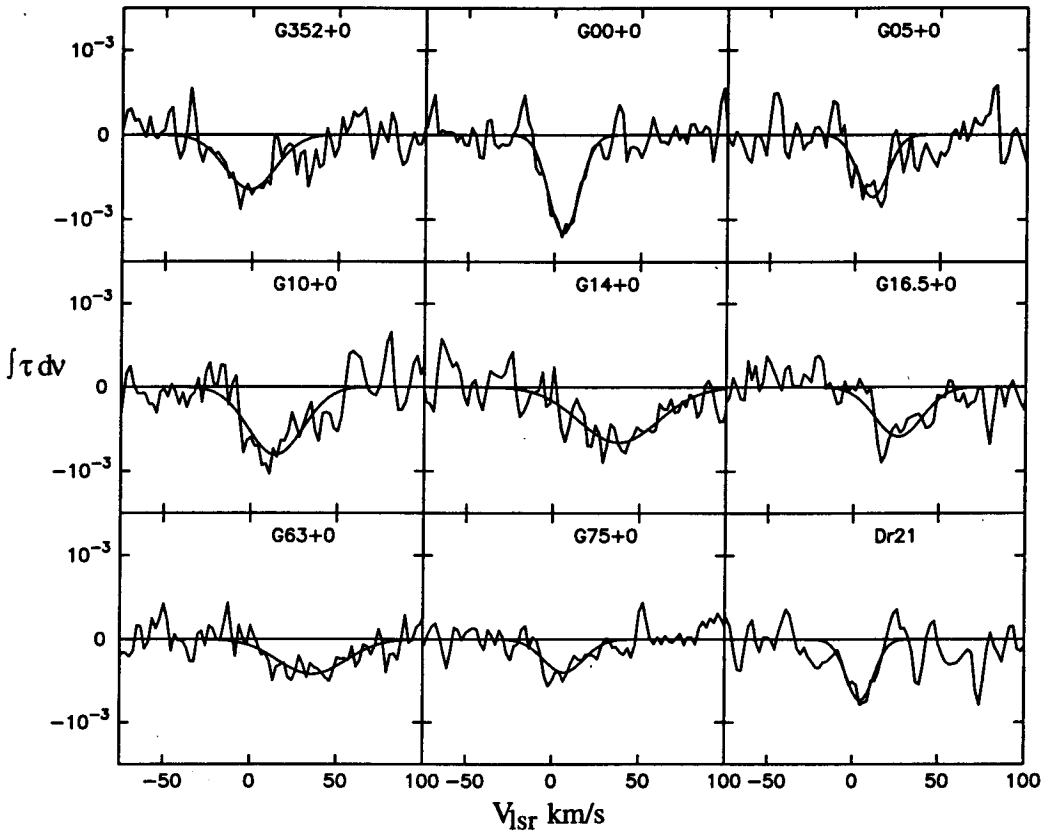

Figure 1. Carbon recombination lines detected near 34.5 MHz ($n \sim 575$). The smooth curve superposed on the observed spectrum is the Gaussian fit to the line profile.

examined for the presence of a spectral feature. A few of the spectra seem to suggest the presence of a weak signal *e.g.*, G342+00, G55+00 and G99+00. However further observations are required to confirm these.

2.2 *Ooty observations near 328 MHz*

The observations with the ORT (Swarup *et al.*1971) were carried out in two sessions: March–April 1995 and October 1995. The ORT is a 30m×530m (EW × NS) parabolic cylinder with an equatorial mount. The length of the telescope along the NS is divided into 11 north and 11 south modules. Since the main aim of these observations was to search for the emission counterpart of the carbon lines seen at 34.5 MHz, a subset of the positions observed at 34.5 MHz were observed with the ORT. Since the size of the carbon line-forming regions is not known, we undertook observations in two modes of operation of the ORT which yielded two different angular resolutions ($\sim 2^\circ \times 6'$ and $\sim 2^\circ \times 2^\circ$ at zenith).

In the first mode, 12 positions were observed with the resolution of the entire telescope (*i.e.* $\sim 2^\circ \times 6'$) whereas in the second mode, 10 of these positions were investigated with the resolution of a single module (*i.e.* $\sim 2^\circ \times 2^\circ$). The telescope

Table 2. Parameters of the lines detected at 34.5 MHz. ΔV is the FWHM. The quoted uncertainties are 1σ.

No.	Source	T_l/T_{sys} $\times 10^{-3}$	V_{lsr} kms^{-1}	ΔV kms^{-1}	$\frac{\int T_l d\nu}{T_{sys}}$ s^{-1}	T_{rms}/T_{sys} $\times 10^{-3}$
1	G352+0	−0.65(0.07)	−1.2(1.8)	34.8(2.6)	−3.3(0.3)	0.21
2	G00+00	−1.16(0.09)	5.3(0.8)	20.5(1.1)	−3.5(0.3)	0.21
3	G05+00	−0.74(0.10)	10.2(1.4)	21.2(2.0)	−2.3(0.3)	0.26
4	G10+00	−0.81(0.08)	14.3(1.7)	37.5(2.5)	−4.3(0.2)	0.29
4a	G10+00	−0.93(0.10)	9.6(1.5)	24.9(2.3)	−4.7(0.4)	0.28
		−0.47(0.11)	40.2(2.6)	18.4(3.7)		
5	G14+00	−0.66(0.07)	37.8(2.7)	54.0(3.8)	−5.1(0.4)	0.22
6	G16.5+0	−0.59(0.07)	26.4(2.0)	32.8(2.8)	−2.8(0.3)	0.22
7	G63+00	−0.42(0.06)	36.2(3.2)	46.0(4.5)	−2.8(0.4)	0.21
8	G75+00	−0.40(0.05)	6.9(1.8)	27.1(2.6)	−1.5(0.2)	0.18
9	DR 21	−0.74(0.13)	4.5(1.6)	18.8(2.2)	−2.0(0.3)	0.26

was used in the total power mode and each position was observed for at least 6 hours. In the higher resolution mode, data are collected simultaneously from two beams (which are labelled beams 5 and 7), separated by 6.6' in declination. Four successive recombination line transitions (C270α to C273α) were observed simultaneously from both the beams using a dual 4-line receiver developed for Galactic recombination line observations (Roshi & Anantharamaiah 2000). The four transitions were averaged to get the final spectra, which on the average have an effective integration time $\sim$ 30 hours. A spectral resolution of 2.1 kms^{-1} was obtained for each band after hanning smoothing. All the lines were detected in emission.

Table 3 shows the observational parameters. On the average, the rms noise on the spectra obtained using the full ORT was $T_{rms}/T_{sys} \sim 2 \times 10^{-4}$ and on the spectra obtained using a single module $T_{rms}/T_{sys} \sim 1.5 \times 10^{-4}$.

Totally, 12 positions (see Table 3) were observed near 328 MHz with the ORT. At the higher resolution, lines were detected from seven of these directions whereas in the low-resolution observations, lines were detected from six directions. The line profiles are shown in Fig 2.

The observed spectra were modelled by Gaussian profiles and the parameters

Table 3. Positions searched for carbon recombination lines at 328 MHz using the ORT.

Source	α(1950)	δ(1950)	Full Telescope		Single Module	
			$\frac{T_{rms}}{T_{sys}}$	t_{eff}	$\frac{T_{rms}}{T_{sys}}$	t_{eff}
	hh mm ss	° ′ ″	10^{-3}	hrs	10^{-3}	hrs
G355+00	17 29 54	-33 08 01	0.19	29.0	0.13	34.7
G00+00	17 42 27	-28 55 00	0.16	23.0	0.11	34.5
G05+00	17 54 00	-24 37 59	0.15	20.5	0.13	34.4
G10+00	18 04 47	-20 17 51	0.17	25.7	0.13	37.1
G14+00	18 12 59	-16 48 00	0.20	19.3	0.19	20.1
G16.5+00	18 17 57	-14 36 18	0.19	33.9	0.15	31.2
G30+00	18 43 29	-02 39 48	0.26	16.0	-	-
G50+00	19 21 02	15 02 41	-	-	0.17	28.2
G62+00	19 46 15	25 29 40	0.19	26.1	0.15	33.9
W49	19 08 51	09 02 27	0.20	20.7	0.17	42.9
W51	19 20 17	14 02 01	0.20	14.5	0.15	26.5
G75+00	20 19 02	36 26 46	0.20	30.7	-	-
NGC2024	05 39 11	-01 55 50	0.20	14.5	-	-

are listed in Table 4. The carbon lines detected in the Galactic plane are broader ($\Delta V \geq 20$ kms^{-1}) and weaker as compared to those detected towards Cas A (Payne *et al.*1989) at this frequency. The lines detected using the full ORT and using the single module had comparable strengths as is evident in Fig 2. No carbon line was detected towards other directions and the rms noise on the spectra are listed in Table 3.

2.3 *VLA observations at 332 MHz*

Observations made with the ORT with two different angular resolutions, provided some preliminary information regarding the angular size of the line-forming region. To obtain constraints on the possible clumpiness of the line-forming gas, we used the VLA to observe the carbon line emission near 332 MHz (270α) towards one of the positions in the Galactic plane which was detected with the ORT. The direction towards Galactic longitude 14° in the Galactic plane was observed for 4.5 hours in June 1995 using the D-configuration of the VLA. Details of this observation are given in Table 5. An amplitude calibrator was observed at the start of the observations. The phase calibrator which was also used for bandpass calibration, was observed once every 30 minutes. The four-IF mode of the correlator which consisted of two circular polarisations (Stokes RR and Stokes LL) and two IF frequencies, was used. Two recombination line transitions (270α & 271α) were observed simultaneously.

Table 4. Parameters of the carbon lines observed with the ORT. ΔV is the FWHM of the line. The numbers in the brackets are the 1σ uncertainty.

Source	T_l/T_{sys} $\times 10^{-3}$	V_{lsr} kms^{-1}	ΔV kms^{-1}	$\frac{\int T_l d\nu}{T_{sys}}$ s^{-1}
		ORT Beam 7		
G355+0	0.2(0.02)	-17.6(3.0)	45.0(7.1)	10.5(2.5)
G00+00	0.65(0.07)	-3.4(0.5)	18.7(1.1)	14.2(2.6)
G05+00	0.4(0.03)	10.7(0.8)	24.2(1.9)	11.1(1.0)
G10+00	0.3(0.02)	20.1(1.3)	32.8(3.0)	11.1(1.2)
G14+00	0.3(0.02)	27.7(1.0)	31.9(2.3)	10.9(0.9)
G16.5+0	0.2(0.02)	32.7(2.3)	39.1(5.3)	9.1(2.3)
G30+00	< 0.15	-	6.2	< 1.1
W49	0.3(0.06)	42.2(1.5)	30.7(3.6)	10.7(2.4)
W51	< 0.12	-	6.2	< 1.1
G62+00	< 0.14	-	6.2	< 1.2
G75+00	< 0.12	-	6.2	< 1.1
NGC2024	< 0.11	-	6.2	< 1.1
		ORT Beam 5		
G355+0	0.2(0.04)	-8.8(1.9)	21.9(4.4)	5.1(2.5)
G00+00	0.61(0.07)	-4.1(0.5)	20.6(1.1)	14.8(1.8)
G05+00	0.5(0.03)	12.3(0.6)	19.0(1.4)	10.9(0.9)
G10+00	0.4(0.02)	20.3(0.8)	29.9(2.0)	13.7(1.1)
G14+00	0.5(0.06)	24.6(1.7)	32.7(3.9)	18.8(1.2)
G16.5+0	0.45(0.1)	20.3(1.4)	11.4(3.3)	6.5(0.8)
G30+00	< 0.20	-	6.2	< 1.5
W49	< 0.17	-	6.2	< 1.2
W51	< 0.14	-	6.2	< 1.2
G62+00	< 0.13	-	6.2	< 1.1
G75+00	< 0.19	-	6.2	< 1.4
NGC2024	< 0.11	-	6.2	< 1.1
		ORT Single Module		
G355+0	0.3(0.02)	0.8(0.7)	20.1(1.7)	6.9(0.7)
G00+00	0.43(0.05)	0.5(0.6)	27.0(1.5)	13.5(1.8)
G05+00	0.52(0.02)	8.2(0.4)	16.2(0.9)	9.8(0.6)
G10+00	0.26(0.02)	21.7(1.2)	36.3(2.9)	10.7(1.0)
G14+00	0.2(0.04)	36.5(3.7)	54.6(8.7)	12.7(4.1)
G16.5+0	0.48(0.07)	20.0(0.8)	12.7(2.0)	7.0(0.6)
W49	< 0.10	-	6.2	< 1.0
G50+00	0.2(0.02)	50.5(1.9)	35.4(4.6)	8.3(2.5)
G62+00	<0.42	-	8.0	<3.7

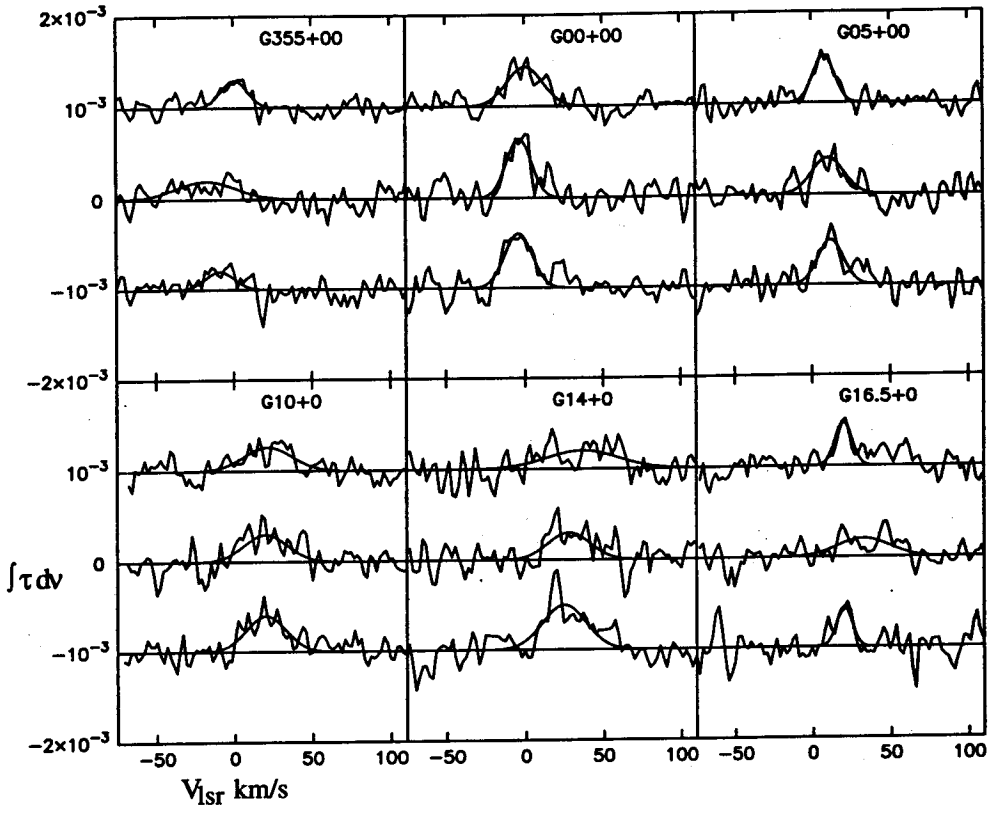

Figure 2. Spectra of carbon lines detected near 327 MHz using beam 5 and beam 7 of the full ORT and using a single module of the ORT are shown. In each frame, the lowermost spectrum is from beam 5 and uppermost is from a single module. These two spectra are offset along the y-axis from their zero-position. The vertical scale applies to all these spectra. The jagged line is the observed spectrum and the smooth line superposed on it is the Gaussian fit to the profile.

The UV data were processed using the standard procedures in the Astronomical Image Processing System (AIPS) developed by NRAO. The continuum image was generated by averaging the visibilities in the central three-quarters of the band. Natural weighting of the data gave a beam size of $5.4' \times 3.5'$ with P.A.$= 1.5°$. A line cube was obtained by Fourier transforming the residual visibilities after subtracting the continuum. To obtain the maximum possible signal-to-noise ratio, natural weighting was applied to the visibilities. Although we aimed at achieving an rms noise of 7-8 mJy/beam in the line images, severe problems due to interference forced us to discard more than 50 % of the data. The rms noise on the line images that we finally obtained was 25 mJy/beam.

The 2° field centred on $l = 14°, b = 0°$ which was imaged using the VLA at 332 MHz is shown in Fig. 3 (a). The rms noise in the image is 150 mJy/beam.

Table 5. Parameters of VLA observations.

Field Centre: $\alpha(1950)$	$18^h12^m59^s$
$\delta(1950)$	$-16°48'03''$
Observing Epoch	June 1995
Duration of Observations	4.5 hours
Observed Transitions	270α, 271α
Rest Frequencies (Carbon)	332.419 MHz
	328.76 MHz
Primary Beam	150'
Shortest spacing	0.035 km
Longest spacing	1.03 km
Observing Mode	4IF
Total bandwidth	781 kHz
	(693 kms^{-1})
Number of Channels	64
Frequency Resolution	12.207 kHz
Velocity Resolution	11 kms^{-1}
Amplitude Calibrator	3C286
Phase Calibrator	1827-360
Bandpass Calibrator	1827-360
Synthesized beam	321.4"×209"
(natural weighting)	
Rms noise, line	25 mJy/beam
Rms noise, continuum	150 mJy/beam

M17 (the bright source at the bottom-left corner of the image), a H II region, is the brightest source in the 2° field with a peak brightness of 40 Jy/beam. The central regions of this nebula are optically thick at low frequencies. The observed brightness temperature at 330 MHz indicates an electron temperature of 7885 °K for the peak emission of M17. which is comparable to the value 8000 K obtained by Subrahmanyan & Goss (1996). Counterparts of other features in Fig. 3 (a) are identifiable on the 5 GHz (Altenhoff *et al.*1979) and 2.7 GHz (Reich *et al.*1990) continuum maps.

The line images showed no emission to a 3σ limit of 75 mJy beam^{-1}. In Fig. 3 (b), the line emission integrated over the ORT beam and divided by the integrated continuum flux (19 Jy) is shown. No line emission is seen in the spectrum and the upper limit on the line-to-continuum ratio of carbon and hydrogen lines is 7.8×10^{-3} (3σ limit). This upper limit is consistent with the ORT results. The VLA observations place a lower limit of 10′ on the size of 'clumps', if any, in the ORT beam. This inference follows from a comparison of the results by Anantharamaiah (1985) who detected the C272α line with a peak flux of 160 mJy using a 2° × 6′

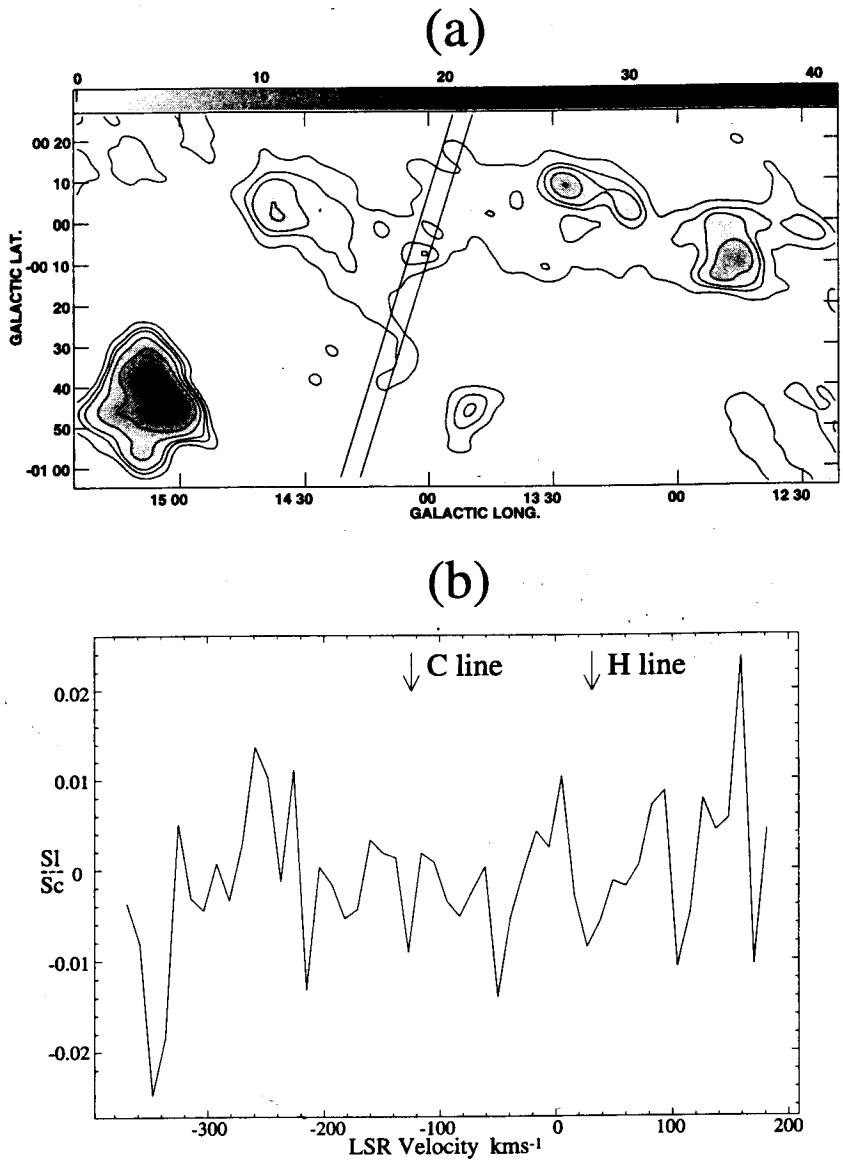

Figure 3. (a) VLA Continuum Image of G14+00 at 330 MHz in Galactic coordinates. The contour levels are 1,3,5,10,20,50,100,110 in units of 0.4 Jy/beam and the grey scale flux ranges from 0 to 41 Jy/beam. The full-ORT beam has been superposed on the continuum map. (b) Spectrum showing the line emission over the full-ORT beam. The arrows show the expected positions of the carbon and hydrogen recombination lines.

beam and the 3σ detection limit of 75 mJy obtained from the present VLA data with a beam of $5.4' \times 3.5'$.

3. Constraints on the physical properties of the carbon line regions

3.1 *Angular size of the line forming regions*

Since the interpretation of the observed recombination lines, in terms of the physical properties of the gas in which they arise, depends sensitively on the fraction of the beam that is filled by the thermal gas, it is necessary to obtain a preliminary idea of its angular distribution. Our observations have been made at different angular resolutions ranging from $21' \times 25°$ at 34.5 MHz to $2° \times 2°$ at 328 MHz and we also make use of the line data at 76 MHz (Erickson *et al.*1995) with a resolution of $4° \times 4°$. Unless the line radiation fills the beam or the distribution of the continuum intensity is highly concentrated and dominates the system temperature (*e.g.* Cas A), beam dilution effects will be significant, and the actual line optical depths will be very different from the apparent (observed) optical depths. Comparison of the line-to-continuum ratios integrated over the width, observed with the two different angular resolutions at 328 MHz (see Table 4) shows that, within the errors, the two ratios are almost equal for most of the positions. This equality indicates that the angular extent of the cloud giving rise to these lines in the inner Galaxy is $\geq 2°$ for most lines of sight. However, the possibility that the line-forming regions are made of a number of nearly uniformly distributed clumps within the field of view is not ruled out by the ORT observations. The VLA observations have placed a lower limit of $10'$ on the size of 'clumps', if any, in the ORT beam.

From their observation of carbon lines near 76 MHz as a function of Galactic latitude, Erickson *et al.*(1995) concluded that the angular extent of the carbon line-forming regions in the inner Galaxy must be approximately 4°. Very low-frequency (near 25 MHz) observation towards $l = 75°$ in the Galactic plane (Konovalenko 1984a) has also indicated that the carbon line-producing region is $\geq 4°$ in extent.

Thus, from the existing observational data on low-frequency carbon recombination lines, it appears that the ionized carbon gas is distributed in form of clouds or clumps with individual sizes $> 10'$ and with an overall extent of at least a few degrees.

3.2 *Constraints from the observed line widths*

One notable difference between the carbon lines observed towards Cas A and the lines observed from positions in the Galactic plane is the width of the lines (Table 6). While the lines detected towards Cas A (last row of Table 6) are seen to broaden with increase in quantum number, which is a clear indication of pressure & radiation broadening, no such trend is seen in the lines observed from the Galactic plane.

The lack of $n-$dependent line broadening towards the Galactic plane seems to

Table 6. Widths of carbon recombination lines observed at different frequencies.

Position	n∼686 25 MHz kms^{-1}	n∼575 34.5 MHz kms^{-1}	n∼443 76 MHz kms^{-1}	n∼271 328 MHz kms^{-1}
G352+0	-	36.4(3.6)	11(1)	20.1(1.7) (G355+00)
G00+00	-	20.5(1.2)	24(1)	27.0(1.5)
G05+00	-	21.0(2.5)	25(4) (G06+00)	16.2(0.9)
G10+00	-	37.0(3.2)	26(2)	36.3(2.9)
G14+00	-	56.0(4.5)	25(3)	54.6(8.7)
G16.5+0	-	32.6(3.4)	47(4)	12.7(2)
G63+00	-	45.9(4.4)	-	-
G75+00	15(0.9)[1]	24.4(2.8)	-	-
DR21	42(12)[2]	18.5(2.7)	-	-
Cas A	71.9(16.4)[3]	26.0(3.1)	6.7(0.4)[4]	5.0(0.5)

[1] From Konovalenko (1984a).
[2] From Golynkin & Konovalenko (1991).
[3] From Konovalenko (1984b).
[4] From PAE89.

indicate that lower electron densities and weaker ambient radiation fields prevail here compared to those in front of Cas A. However, the observed widths ($\geq$ 20 kms^{-1}) of the lines from the Galactic plane cannot be explained by thermal motions and micro-turbulence ($\sim$ few kms^{-1}) in the cool clouds. We suggest that the lines are broadened by the systematic motions owing to differential Galactic rotation and hence lack an $n-$dependence.

Since pressure (ΔV_P) and radiation (ΔV_R) broadenings are expected to be maximum at 34.5 MHz, the line widths at this frequency can be used to derive upper limits on the electron density and the ambient radiation field. We used Equations (1) and (2) from the paper by Shaver (1975) for deriving the limits which are listed in Table 7; and we reproduce them below for ready reference

$$\Delta V_P = 2 \times 10^{-8}\, exp\left(-\frac{26}{T_e^{1/3}}\right) \frac{n_e n^{5.2}}{T_e^{1.5}} \frac{c/(kms^{-1})}{\nu/(kHz)} \quad \text{kms}^{-1} \qquad (1)$$

$$\Delta V_R = 8 \times 10^{-20}\, W_\nu\, T_{R,100}\, n^{5.8} \frac{c/(kms^{-1})}{\nu/(kHz)} \quad \text{kms}^{-1} \qquad (2)$$

where ΔV_P and ΔV_R are the FWHM due to pressure and radiation broadening (kms$^-$1), T_e is the electron temperature (K), n_e is the electron density (cm^{-3}), n is the quantum number, c is the velocity of light (kms^{-1}), ν is the frequency (kHz), W_ν is the dilution factor, $T_{R,100}$ is the radiation temperature (K) at 100 MHz.

Table 7. Upper limits on the electron density and radiation temperature (at 100 MHz) from the observations at 34.5 MHz.

Position	ΔV_{obs} kms^{-1}	$n^1_{e,max}$ cm^{-3}	$T^1_{R100,max}$ K	T^2_{R100} K	ΔV^3_{exp} kms^{-1}
G352+00	36.4(3.6)	1.21(0.12)	5160(510)	3460	24.4
G00+00	20.5(1.2)	0.68(0.04)	2906(170)	5030	35.5
G05+00	21.0(2.5)	0.7(0.08)	2977(354)	5030	35.5
G10+00	37.0(3.2)	1.23(0.11)	5245(454)	5660	40.0
G14+00	56.0(4.5)	1.86(0.15)	7938(638)	5660	40.0
G16.5+0	32.6(3.4)	1.08(0.11)	4621(482)	5030	35.5
G63+00	45.9(4.4)	1.51(0.15)	6507(624)	2830	20.0
G75+00	24.4(2.8)	0.81(0.09)	3459(370)	2830	20.0
DR21	18.5(2.7)	0.61(0.09)	2622(383)	2680	19.0

[1] Upper limit derived from the observed line width at 34.5 MHz and using $T_e = 20$ K and $W_\nu = 1$.
[2] Averaged value over the Gauribidanur beam of 25° obtained from the continuum map at 34.5 MHz (Dwarakanath 1989) and extrapolated to 100 MHz using a spectral index $\alpha = 2.6$ where $T_B \propto \nu^{-\alpha}$.
[3] Expected line broadening at 34.5 MHz due to T_{R100} noted in column 6 and assuming $W_\nu = 1$.

The widths listed in Table 7 were calculated assuming that the entire width is due to either of the broadening mechanisms. The upper limits on the electron density in the medium were calculated for a nebula at 20 K.

The insignificant contribution of pressure and radiation broadening to the line width at 34.5 MHz indicates that the actual electron densities and radiation fields are much smaller than those listed in columns 4 and 5 of Table 7. Furthermore, the electron density decreases if the kinetic temperature is increased *e.g.* the values of n_e noted in column 4 will decrease by a factor of ~ 4 if T_e increased to 75 K. The derived upper limit for the radiation temperature in the Table assumes a dilution factor of unity which implies that the absorbing cloud is isotropically illuminated by the non-thermal radiation field. The actual radiation temperature seen by the cloud could be equal to or less than the values listed in column 6, which were obtained from the $26' \times 42'$ continuum map of Dwarakanath (1989) at 34.5 MHz. The widths of the carbon lines near 34.5 MHz as predicted by this radiation field are listed in column 7.

The limits listed in Table 7 are useful because they define the absolute boundaries of the parameter space that we use for modelling the observed recombination lines.

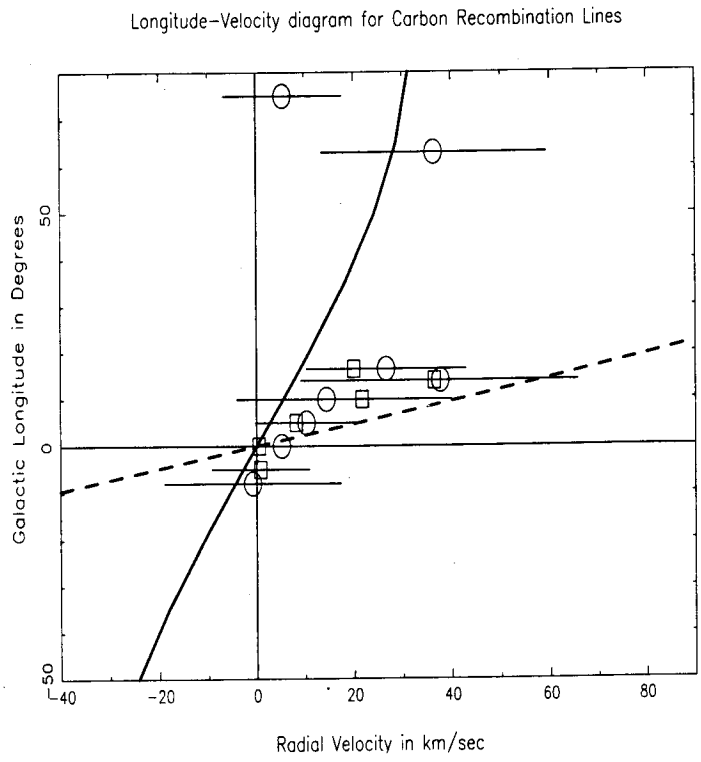

Figure 4. The Longitude-Velocity diagram of the carbon recombination lines at 34.5 MHz(circles) and 328 MHz(squares) from the Galactic plane. The horizontal lines about each point represent the observed widths of the lines. The solid line shows the variation of the radial velocity with longitude for a cloud placed at a Galactocentric distance of 7.5 kpc whereas the dashed line shows the expected l-v plot for a cloud at a distance of 4 kpc. These are obtained using the Galactic rotation model of Burton (1988).

3.3 *Longitude-Velocity diagram*

The l-v diagram for the carbon recombination lines observed at 34.5 and 328 MHz is shown in Fig. 4. The Galactic rotation model by Burton (1988) has been used. The kinematic nature displayed by gas at Galactocentric distances of 7.5 kpc (solid line) and 4 kpc (dashed line) is also shown in the figure.

All the observed points with $l > 0°$ lie between 4 and 7.5 kpc. This range coincides with the regions observed to be rich in molecular clouds (Scoville & Solomon 1975), H166α emission (Lockman 1976) and strong H II regions (Downes *et al.*1980). Broad lines of H I emission (Burton 1988) and absorption (Garwood & Dickey 1989), ^{12}CO (Bania 1977), H166α (Lockman 1976) and [C II] 158 μm (Mizutani *et al.*1994) emission are observed towards the Galactic centre. These broad (> 100 kms^{-1}) lines are due to non-circular motions near the Galactic centre. However, the low-frequency carbon recombination lines observed by us are relatively narrow (~ 20 kms^{-1}). The hydrogen recombination lines near 327 MHz observed by Anantharamaiah (1985) and Roshi & Anantharamaiah (1997) are also relatively narrow. Excluding the Galactic centre direction, the l-v distribution of

the carbon lines that we observe resembles that traced by H I absorption, diffuse H II (Lockman *et al.*1996) and ^{12}CO (except for the features due to the 3 kpc arm). Erickson *et al.*(1995) have a more continuous sampling of carbon lines near 76 MHz ($n \sim 445$) in the inner Galaxy and they also find that the gas responsible for the lines lies between galactocentric distances of 5 and 8 kpc. With the available data, we can only say that the gas giving rise to carbon lines in the inner Galaxy is likely to be distributed between galactocentric distances of 4 and 8 kpc and is likely to be associated with either the cold H I gas, or the molecular gas or the H II regions. From the similarity of the $l-v$ distributions of the emission lines observed near 328 MHz and the absorption lines detected near 34.5 MHz and 76 MHz from the inner Galaxy ($l < 17°$), we assume that all these lines arise in the same ionized carbon gas.

3.4 *Origin of carbon lines in cold, neutral gas*

Although the widths of the observed lines do not rule out an origin in classical H II regions, the low electron densities (previous section) and the absence of hydrogen recombination lines at low frequencies rule out such an origin. Hence, the lines are most likely associated with cold gas where only carbon is ionized. The possibilities are either the atomic H I gas (the cold neutral medium), the molecular gas or the low-excitation photodissociation regions in the interstellar medium. Interpretation of low-frequency recombination lines observed towards the direction of Cas A has shown that these lines are most likely to be associated with atomic H I gas. However, the different pressure and radiation broadening seen in the low-frequency lines observed from Cas A and the Galactic plane suggests that detectable low-frequency lines may arise in regions with a range of physical properties. In a review paper, Sorochenko (1996) discusses Cas A and other such directions towards which carbon lines have been detected and concludes that C II regions are formed on the surface of molecular clouds exposed to external ionizing UV radiation either close to H II regions or around isolated molecular clouds.

4. Modelling the line-forming regions

4.1 *Assumptions of the model*

We assumed a cloud of uniform density n_e , temperature T_e and emission measure EM illuminated by a non-thermal radiation field characterized by a brightness temperature T_{R100} at 100 MHz. Although this is a simplified model and the real cloud is likely to contain density condensations, it can be used to derive the average properties of the medium under consideration. The solution of the radiative transfer equation is (Shaver 1975):

$$T_l = T_o \left[e^{-\tau_c}(e^{-b_n\beta_n\tau_l^*} - 1)\right] + T_e \left[\frac{(b_n\tau_l^* + \tau_c)}{\tau_l + \tau_c}(1 - e^{-\tau_l+\tau_c}) - (1 - e^{-\tau_c})\right]. \quad (3)$$

In Equation (3), T_l is the line temperature, T_o is the background temperature, T_e is the electron temperature, τ_c is the continuum optical depth at the given frequency, τ_l^* is the LTE line optical depth, τ_l is the non-LTE line optical depth and b_n and β_n are the departure coefficients which measure the deviation of the level populations from LTE values. Further simplifying assumptions which approximate the real system are made. At low frequencies, the lines are sensitive to tenuous, cool nebulae *i.e.* $T_e << T_o$. Since $\tau_c, \tau_l << 1$ at these frequencies, the second term in the above equation is much smaller than the first term and can be neglected. Hence, the line temperature can be expressed under these conditions as:

$$T_l = T_o \left[e^{-\tau_c}(e^{-b_n\beta_n\tau_l^*} - 1)\right]. \quad (4)$$

Since $T_c = T_o\, e^{-\tau_c}$ and $\tau_c << 1$, the line-to-continuum ratio can be approximated as

$$\frac{T_l}{T_c} = -b_n\beta_n\tau_l^* = -\tau_l. \quad (5)$$

The departure coefficients b_n and β_n quantify the non-LTE effects influencing the level populations. The true population of a level n is given as $N_n = b_n N_n^*$ where N_n^* is the expected LTE population. $\beta_n = 1 - \frac{kT_e}{h\nu}\frac{d(lnb_n)}{dn}$ depends on the gradient of b_n with n. A negative value of β_n signifies inverted populations and hence stimulated emission. A positive value of β_n means that the line at that frequency is likely to appear in absorption if the background temperature $T_o > T_e$. The RHS of Equation (5) is the non-LTE value of the line optical depth.

Rewriting Equation (5) in terms of antenna temperatures:

$$\tau_l = \frac{\Omega_c}{\Omega_L}\,\frac{T_{A,l}}{T_{A,c}} \quad (6)$$

where Ω_c, Ω_l are the solid angles subtended by the continuum and the line-forming regions. $\Omega_c, \Omega_l \leq \Omega_B$ where Ω_B is the solid angle subtended by the telescope beam. $T_{A,l}$ and $T_{A,c}$ are the line and continuum antenna temperatures. At 34.5MHz, the non-thermal background radiation dominates the continuum temperature. Since this background is all-pervasive in the Galaxy, $\Omega_c \geq \Omega_B$ and the main factor responsible for the unknown beam dilution factor is the extent of the line-forming gas within the observing beam.

At low frequencies, line-widths are likely to be affected by various n-dependent line broadening mechanisms, leading to reduction in the peak optical depths and increased widths. Therefore, the integrated optical depth is the correct physical quantity to compare at different frequencies. Theoretically, the integral of the line optical depth can be written as (Payne *et al.*1994):

$$\int \tau_l d\nu = 2.046 \times 10^6 \; T_e^{-5/2} e^{\chi_n} \; EM_l \; b_n \beta_n \quad s^{-1}. \tag{7}$$

Using this Equation, we attempt to fit the observed variation in the integrated optical depth given by Equation (5) with principal quantum number for plausible combinations of T_e and n_e .

4.2 *The modelling procedure*

We use carbon line observations at three frequencies to model the C II regions– our observations at 34.5 MHz and 328 MHz and the Parkes observations by Erickson *et al.*(1995) at 76 MHz. The angular resolution of these observations are different. We assume that the lines at the three frequencies arise in the same gas.

Each model is characterized by an electron temperature T_e, electron density n_e, emission measure EM, radiation temperature T_{R100} , carbon depletion factor δ_C and the angular size of the line-forming region. As discussed earlier, the upper limits on T_{R100} and n_e were determined from the widths of the lines observed at 34.5 MHz. We consider a range of possible temperatures for the line-forming region which include the typical temperatures of cold H I , H_2, and photo-dissociation regions which are all probable places of origin for the carbon lines. The lower limit on the electron densities is set from the maximum pathlengths through the Galaxy. We considered models with a carbon depletion factor of 0.5. Since observations indicate that the line-forming region could have an angular size $\geq 2°$, we explore models in which the line-forming region is (a) ubiquitous (*i.e.* fills all the beams that are used); (b) 4° and (c) 2°. The departure coefficients b_n and β_n which account for the non-LTE effects were calculated using the computer code, originally due to Salem & Brocklehurst (1979) and later modified by Walmsley & Watson (1982) and Payne *et al.*(1994).

The model integrated optical depths are calculated for different n using Equation (7) and the models are normalized to the observed integrated optical depth at 328 MHz. The ratio of line temperature to system temperature is considered to be equivalent to the line-to-continuum ratio, since the system temperature is dominated by the strong sky background at these low frequencies. Any model that we generate needs to satisfy the observed integrated optical depth $\frac{\int T_l d\nu}{T_{sys}}$ and be consistent with the upper limits on the physical conditions placed by the line data at 34.5 MHz. Since the observed width of the line is independent of frequency, we assumed that the contribution to the width at 34.5 MHz due to pressure broadening is < 5 kms^{-1} . This assumption translated to an upper limit on the electron density of 0.3 cm^{-3}. The lower limit was 0.001 cm^{-3}. The electron temperature space was varied from 20 K to 400 K. These models were generated for two values of the radiation temperature at 100 MHz which were 1250 K and 2500 K.

The non-LTE population is calculated assuming that the quantum levels are in statistical equilibrium so that the rate of population of a level n due to all possible physical processes is equal to the rate of depopulation of that level (Shaver 1975).

The main physical processes which determine the level populations are collisional and radiative excitation and de-excitation. The departure coefficients are calculated by solving a series of differential equations after imposing a boundary condition $b_n \rightarrow 1$ as n $\rightarrow \infty$ (Salem & Brocklehurst 1979) *i.e.* the levels are assumed to be in LTE at very large n. In case of carbon, it is necessary to also consider a dielectronic-like recombination process which significantly influences the high-n populations if the temperatures are around 100 K (Watson *et al.*1980)

4.3 *Results of modelling*

We examine the models which explain the observed variation in the integrated optical depth with frequency. The criteria used to select the possible physical models are (a) the observed behaviour of the integrated optical depth as a function of n, (b) the path lengths through the region which should be $\leq$ 5 kpc, as required by the observed line widths and (c) the turnover from emission to absorption which should occur at $n < 443$ as the lines are observed in absorption at 76 MHz (Erickson *et al.*1995). We classify the results on the basis of the assumed angular size of the line-forming regions. The angular size determines the beam dilution and the scaling from the observed to true optical depth. The data at the three frequencies have different angular resolutions and therefore different beam-filling factors. In all the cases, we assume, for simplicity, that the non-thermal radiation field uniformly fills the beams.

4.3.1 *Case 1: Cloud size > 4° or equal beam coverage by line and continuum*

We found that remarkably similar physical models reasonably explained the observed data towards the six positions in the inner Galaxy. The best-fitting models towards three of the positions, $l = 0°$, $l = 5°$, and $l = 14°$ are shown in Fig. 5 (panels on left) and the parameters are listed in Table 8(a). In all these models, we assumed $T_{R100} = 1250$ K. Similar physical properties were found if $T_{R100} = 2500$ K. All the models were constrained by the data at 328 MHz. The turnover from emission to absorption occurs around $n \sim 400$. We found no model which simultaneously explains the data at 76 MHz and 34.5 MHz, which is most likely due to the unknown beam dilution at 34.5 MHz. The models which explained the observed variation in $\frac{\int T_l d\nu}{T_{sys}}$ with n were within the temperature range $20 - 40$ K. Outside this range, the models predicted large optical depths at 76 MHz and 34. 5 MHz. The electron densities in the acceptable models are 0.1 cm^{-3}. Although higher electron densities provided better fits to the data (e.g. the dashed line in Fig. 5 for G00+00 has $n_e = 0.3$ cm^{-3}), the resulting collisional broadening at 34.5 MHz exceeded the limit of 5 kms^{-1} and hence are not favoured.

The path lengths through the cloud range from 0.07 pc to 0.9 pc suggesting a sheet-like morphology for the regions and the emission measures are $\leq$ 0.01 pc cm^{-6}. Typical pressures in terms of $n_H T_e$ are a few tens of thousands cm^{-3}K,

Table 8. Model parameters for three positions for three assumed cloud sizes. T_{R100} = 1250 K.

Position	T_e K	n_e cm^{-3}	EM $pccm^{-6}$	$Size$ pc	$n_H T_e$ $cm^{-3}K$
		(a) Cloudsize > 4°			
G00+00	40	0.1	0.009	0.9	26680
	20	0.3	0.006	0.07	40000
G05+00	20	0.1	0.002	0.2	13340
	40	0.1	0.007	0.7	26680
G14+00	40	0.1	0.007	0.7	26680
		(b) Cloudsize = 4°			
G00+00	80	0.03	0.019	21.1	16000
	200	0.03	0.079	87.8	40000
G05+00	60	0.05	0.01	4.0	19980
	80	0.03	0.014	15.6	16000
G14+00	80	0.03	0.018	20.0	16000
	100	0.03	0.025	27.8	20000
		(c) Cloudsize = 2°			
G00+00	150	0.03	0.051	56.7	30000
	300	0.03	0.151	167.8	60000
G05+00	150	0.03	0.037	41.1	30000
	200	0.03	0.058	64.4	40000
G14+00	200	0.03	0.075	83.3	40000
	300	0.03	0.142	157.8	60000

which is higher than the average thermal pressure in the interstellar medium. We did not find any model which was in pressure equilibrium with HI. The relatively low temperatures in these models suggest association with molecular clouds.

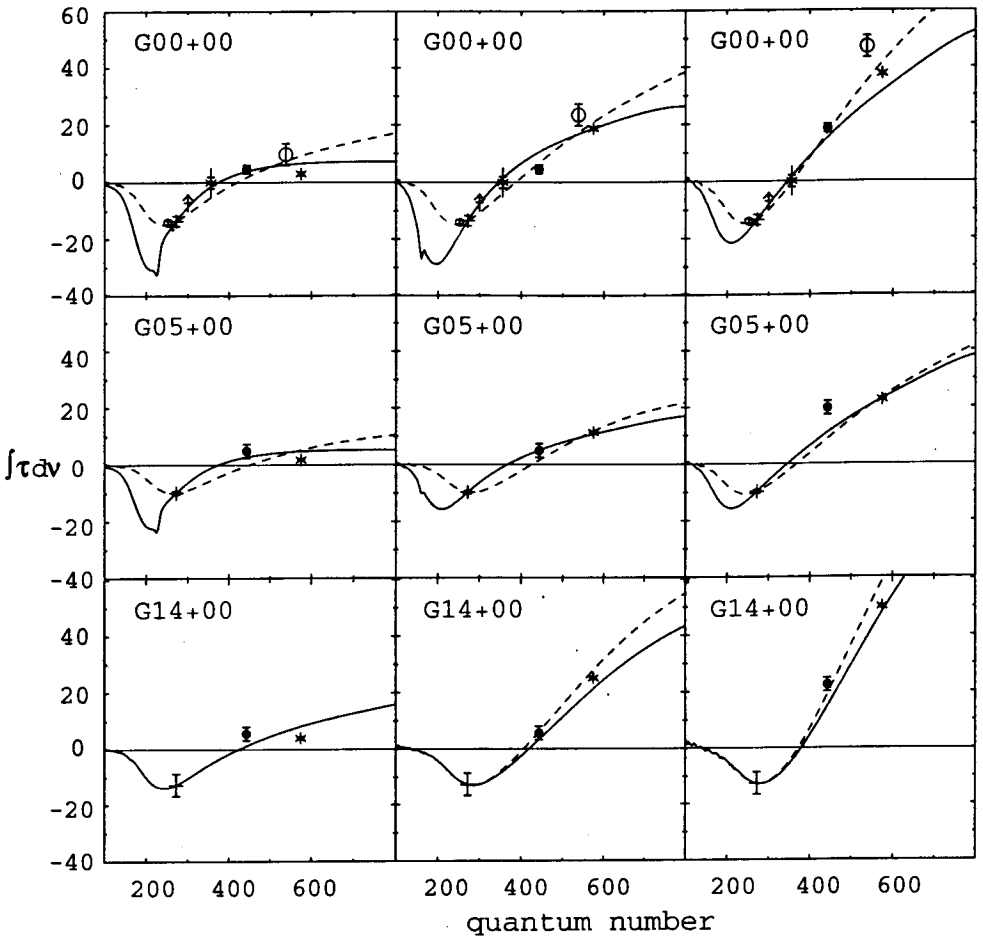

Figure 5. Model fits to observed carbon line data shown for three Galactic plane positions. The unbroken line and broken lines represent the two best-fit models for the two sets of parameters given in Table 8. The left panels show models for clouds assumed to be $\geq 4°$; the centrepanels show model fits for clouds assumed to be $= 4°$; and the panels on the right show models for clouds $= 2°$. Towards G00+00, the $n = 252, n = 300$ points are from Pedlar *et al.*(1978), $n = 356$ is from Anantharamaiah *et al.*(1988) and $n = 530$ is from Smirnov *et al.*(1996).

4.3.2 *Case 2: Cloud size* $= 4°$

These regions, if placed at a radial distance of 3.5 kpc from us, would have a linear size of 250 pc which is comparable to the scale height of the atomic gas. The best-fitting physical models have T_e in the range of $60 - 80$ K, n_e in the range of $0.03 - 0.05$ cm^{-3}, and path lengths range from 4 pc to 30 pc. Fig. 5 (centre panels) shows the models for the positions $l = 0°$, $l = 5°$ and $l = 14°$ and Table 8(b) lists the parameters. All the models are for $T_{R100} = 1250$ K. The turnover from

emission to absorption occurs around $n \sim 400$. The relatively warmer temperatures in these models favour association with atomic H I gas in the Galaxy. However, the thermal pressures are more than 3 times the average interstellar pressure ($n_H T_e \sim 5000$ cm^{-3}K). There was no change in model parameters with $T_{R100} = 2500$ K except for a slight lowering of quantum number at which the turnover occurs.

4.3.3 *Case 3: Cloud size* $= 2°$

If these regions are placed at a radial distance of 3.5 kpc, then their linear size would be ~ 125 pc. Models for three Galactic plane positions are shown in Fig. 5 (panels on the right) and the parameters are listed in Table 8(c). Best-fitting models have T_e between 150 K and 200 K and the electron density $n_e \sim 0.03$ cm^{-3}. Lower temperatures are possible if the upper limit on the electron density is relaxed i.e. the pressure broadening is > 5 kms^{-1} . The path lengths required by these models ranged from 40 to 170 pc. The models with $T_{R100} = 2500$ K slightly lowered the quantum numbers at which the turnover occurs, but the overall model parameters remained similar.

5. Discussion

The modelling described in the previous sections showed that most of the positions within $l = 352°$ to $l = 17°$ possess remarkably similar physical properties. Quantitatively, if the clouds along the line-of-sight are $> 4°$ in extent, then typically $T_e = 20 - 40$ K, $n_e \sim 0.1$ cm^{-3} and the pathlengths are tiny (< 1 pc). On the other hand, if the cloud is $4°$ in size then it is likely to be at a temperature between 60 and 200 K, with electron density between ~ 0.03 and 0.05 cm^{-3}. The path lengths through these clouds are in the range $4 - 90$ pc. If the cloud subtends an angle of $2°$, then they are likely to have $T_e = 150 - 300$ K and $n_e = 0.03$ cm^{-3} and pathlengths between 40 and 170 pc. All these models are able to reasonably explain the observed variation in the optical depth with n. Since the data is limited and the angular resolution is coarse, it is not possible to derive more stringent constraints on the parameters. It is entirely possible that the observed carbon recombination lines arise in clouds possessing a range of temperatures, electron densities and angular sizes. Here we discuss the plausibility of the above models using qualitative arguments.

The low temperature ($T_e = 20$ K) models give a good fit to the observed line strengths at two frequencies for most positions. If these models correctly explain the physical properties of the line-forming regions then their inability to explain the third data point is probably telling us about the beam dilution at the lowest resolution. However, these models require extremely short pathlengths through the ionized carbon gas. Since the widths of the lines detected at frequencies differing by a factor of ~ 10, are found to be very similar, it implies that pressure and radiation broadening, which are strong functions of n is not responsible for the line widths even at the lowest frequency (*i.e.* ~ 34.5 MHz). The origin of the ob-

served width is, most likely, due to the differential Galactic rotation with the gas distributed between galactocentric distances of 4 and 7 kpc. However, the pathlengths required by the low-temperature models are tiny < 1 pc. If this pathlength is to be divided into smaller regions and distributed over ~ 3 kpc (to explain the line width), then it would require individual clouds to be < 0.1 pc thick which implies an extremely thin sheet-like geometry since the angular extent of the clouds is $> 4°$. This peculiar morphology for the clouds makes the models difficult to accept; however they are not entirely implausible. These thin sheet-like structures are reminiscent of ionization fronts near star-forming regions which typically have a thickness of ~ 0.02 pc suggesting a scenario where carbon is photo-ionized in a thin outer layer of molecular clouds by the ambient ultraviolet radiation field. However, to expect many such sheet-like objects to be distributed along every line-of-sight to generate the observed strength and widths appears too contrived. In the case of Cas A (the most-studied direction in recombination lines at low frequencies; Payne *et al.*, 1994 and the references therein), the low$-T_e$ models were ruled out since they failed to explain the observed variation in optical depth. Another interesting difference is that the carbon lines towards Cas A were distinctly affected by frequency-dependent line broadening whereas the lines from the Galactic plane positions hardly show any $n-$dependent broadening suggesting different physical conditions, especially the electron density and radiation field. The main drawback of the data we use here is that they are at only three frequencies, and with different and coarse angular resolutions which makes beam dilution an important issue. In contrast, for the data towards Cas A, the beam-size was determined by the continuum emission from Cas A since it dominates the system noise. One argument in favour of the low-temperature models is that the constraint on pressure equilibrium with the interstellar medium is lifted since the gas is assumed to coexist with molecular gas. Moreover, since the carbon lines seem to be widely detectable in the inner Galaxy, it also favours association with molecular gas which has maximum surface brightness in that region.

The higher temperature ($T_e \geq 60$ K) models, which indirectly assume coexistence of ionized carbon with atomic HI gas in the Galaxy, successfully fit the observed data towards most of the inner Galaxy positions if the angular size of the clouds is $4°$ or $2°$. Due to the low electron densities (~ 0.03 cm^{-3}) in these models, they are sensitive to changes in the radiation temperature. For $T_{R100} = 5500$ K (such high radiation temperatures are ruled out by the observed line widths near 34.5 MHz), data from all the positions could be fitted assuming a cloud size of $4°$ or $2°$, whereas for $T_{R100} = 1250$ K (which produces a radiation width of ≤ 5 kms^{-1} at 34.5 MHz for a dilution factor of 0.5), a few of the positions could not be fitted to the model. With the present data, we cannot obtain a more quantitative interpretation of this result. As mentioned before, the range of physical conditions in the clouds predicted by the warm models appears to be well-constrained. However, we had to relax the criterion of pressure equilibrium with HI to obtain good fits to most of the data. So, all the models in which the temperature favours association with HI have kinetic pressures which range from $3 - 10$ times the interstellar

pressures. These models do predict reasonable pathlengths for the line-forming clouds. Recall that towards Cas A, the warm models (Payne *et al.*1989, Payne *et al.*1994) satisfactorily explained the observed variation in optical depth over a wide frequency range. Thus, we favour the view that a significant fraction of low-frequency carbon recombination lines arise in warm H I gas in the photodissociation regions.

The range of physical parameters that we obtain in this analysis seems to favour an association of the C II gas with the photo-dissociation regions. A photo-dissociation region as defined by Tielens & Hollenbach (1985) are "regions where FUV radiation (6 – 13.6 eV) dominates the heating and/or some important aspect of the chemistry" and contains most of the atomic and molecular gas in the Galaxy. The low-excitation photo-dissociation region discussed by Hollenbach *et al.*(1991) are illuminated by the interstellar radiation field. These regions, according to them, include a warm (T$\geq$ 100 K) atomic region comprised of hydrogen, oxygen and ionized carbon near the surface. Beyond that, is a cool ($T \sim 50$ K) partially dissociated region and still further in the interior is a cooler ($T \sim 10 - 20$ K) region. The photo-dissociation regions encompass a wide range of physical properties. It appears highly probable that carbon recombination lines arise at various depths in the photo-dissociation region. From the present results, it appears that ionized carbon can be distributed in clouds of a range of angular sizes along the line of sight and possess a variety of physical properties resulting in detectable carbon lines.

However, the above argument also raises more questions. If the carbon lines arise in the neutral gas, probably within a low-excitation photo-dissociation region with temperatures ranging from 80 to 300 K (and possibly 20 K), then why are they not detected from many more directions in the Galaxy? It appears reasonable to expect the existence of stronger carbon lines from directions which show high H I optical depth or high ^{12}CO emission. However, this is not always the case. For example, inspite of the large H I optical depth observed towards $l = 30°$ in the Galactic plane, no carbon line near 328 MHz or 34.5 MHz has been detected. Another such interesting direction is towards the extragalactic source 3C 123. Although, this direction shows a high H I optical depth ($\tau_{\rm HI} \sim 2.5$), no carbon recombination line near 318 MHz ($n \sim 274$) (Payne *et al.*1984) have been detected down to an optical depth limit of 3×10^{-4}. Payne *et al.*(1994) explain that this non-detection could be due to the slightly higher temperature of the H I clouds in this direction which renders the lines undetectable. However, from the modelling in the previous section, we find that a range of temperatures (80 – 300 K in the warm models) for the carbon line-forming regions can give rise to detectable peak optical depths of $10^{-3} - 10^{-4}$ for a range of electron densities. If pressure equilibrium with H I gas is assumed, then the models we find have electron densities between 0.005 and 0.007 cm^{-3} implying atomic densities $n_H \sim 50$ cm^{-3}. Larger electron densities ($\sim$ 0.03 cm^{-3}) that we find for the best-fitting models cause the gas to move out of pressure equilibrium with H I. On the other hand, lower electron densities ($n_e < 0.003$ cm^{-3}) require extremely long pathlengths through the ionized-carbon gas to generate the observed line intensities. Therefore, if such electron densities

existed in the ionized-carbon gas then also the recombination lines would be undetectable. Hence it appears that detectablity of the low-frequency recombination lines is a sensitive function of both the electron density and temperature. At this point, it may be useful to note that low-frequency observations have detected carbon lines with line-to-continuum ratios ranging from a few times 10^{-4} to a few times 10^{-3}. It appears certain that lines very much stronger than a few times 10^{-3} are not common. However, the lower limit is set by the sensitivity of the observations conducted till date. Hence, lines intrinsically weaker than few times 10^{-4} might possibly exist and would require more deeper observations to detect them. It therefore appears that with the present sensitivity only a subset of the range of values possible for these parameters has so far been accessible through low-frequency recombination lines of carbon.

The physical properties of the gas in the inner Galaxy are remarkably uniform. Surprisingly, these lines which are so widespread in the inner Galaxy ($l < 17°$) appear to be difficult to detect in the outer Galaxy except towards a few directions ($l = 63°\&75°$). The reason possibly lies in the cloud sizes and also in the reduced background radiation field. Alternatively, since these observations have shown that the clouds in the inner Galaxy are $\geq 2^{\circ}$, the non-detectability could be due to the different physical conditions that may exist in the photo-dissociation regions in the inner and the outer Galaxy. More sensitive multifrequency observations towards several directions in the outer and inner Galaxy are required to ascertain the widespread existence of low$-\nu$ carbon recombination lines.

5.1 *The site of formation of the [*C II *] 158 μm line and the low$-\nu$ carbon recombination lines*

The [CII] 158 μm line is a result of the radiative decay of the fine-structure transition, $^2P_{3/2} \rightarrow {}^2P_{1/2}$ in singly ionized carbon. The recombination lines, on the other hand, are a result of the electronic transitions of an electron which has most likely dielectronically recombined by exciting the same fine structure transition. The two lines are thus, intimately related and it is natural to look for a correlation between the two. However, although dielectronic-like recombination process is one excitation mechanism for the fine-structure line, it is not the only one. Recent advances in infrared observations have extensively detected the [CII] 158 μm line from the Galaxy and it has been inferred that a wide range of physical conditions are conducive to the formation of the fine-structure line. C^+ ions giving rise to the infrared line are found to exist in both neutral and ionized regions. Shibai *et al.*(1991) concluded from their balloon-borne experiments that the diffuse [CII] emission of the Galactic plane comes from the diffuse gas whereas Bennett & Hinshaw (1993) showed that the [CII] emission measured with COBE/FIRAS may originate in the photo-dissociation region. Petuchowski & Bennett (1993) and Heiles (1994), in separate studies, analysed the [CII] data and studied its correlation with the various possible sites of origin. Both the studies find that the extended low-density warm ionized medium which has a temperature around 10^4 K is the main global

contributor to the 158 μm fine-structure emission line, especially in the Galactic interior. Heiles (1994) argues that the next dominant contributor to the infra-red line is the cold neutral medium and the last is the photo-dissociation region. On the other hand, low-frequency carbon recombination line emission is detected only from cold neutral gas and probably molecular gas and not from the extended low-density warm ionized medium. The major contributor to the two species of lines, the C II 158μm and low-frequency carbon recombination lines seem to be different and hence we have not pursued a rigorous treatment of the correlation.

6. Summary

In this paper, we have presented observations of carbon recombination lines at 34.5 MHz and 325 MHz in the Galactic plane. The observations at 34.5 MHz ($n \sim 575$) were conducted using the low-frequency dipole array at Gauribidanur and at 328 MHz ($n \sim 272$) using the Ooty Radio Telescope. Carbon lines were detected from nine out of the 32 directions that were observed at 34.5 MHz. The lines at both the frequencies are weak with line-to-continuum ratios ranging from a few times 10^{-4} to 10^{-3} and line widths of $15 - 50$ kms^{-1} . The similarity of widths observed at the two frequencies suggest that the effect of radiation and pressure broadening is negligible and it is likely that the widths are due to differential Galactic rotation. Observations at 328 MHz, which were made with two angular resolutions, indicate that the angular size of the line-forming gas is $\geq 2^\circ$. Higher resolution VLA observations at 330 MHz towards one of the directions, $l = 14^\circ, b = 0^\circ$ failed to detect any carbon line emission to a 3σ level of 75 mJy beam^{-1}and implies a lower limit of $10'$ on the angular size of any possible clumps in the line-forming regions.

The l-v distribution of the carbon line data indicates that the line-forming regions are located between 4 and 7 kpc from the Galactic Centre. Combining the data at 34.5 MHz and 328 MHz with those of Erickson *et al.*(1995) at 76 MHz obtained using the Parkes telescope, we modeled the line-forming regions. Upper limits on the electron densities and the radiation fields were obtained from the observed line widths at 34.5 MHz. For different assumed angular sizes of the line-forming regions, we found combinations of temperature T_e , density n_e and pathlength l which could satisfactorily explain the observed variation of integrated line optical depth with frequency. The models were found to be sensitive to the assumed size of the line-forming region. In all the models, we assumed that the background continuum radiation uniformly fills the beam. Models were obtained for two values of the background radiation field $T_{R100} = 1250$ K and $T_{R100} = 2500$ K. For an assumed cloud size $> 4^\circ$, we found that the best-fitting parameters are $T_e \sim 20 - 40$ K, $n_e \sim 0.1$ cm^{-3} and $l < 1$ pc. For an angular size of 4°, models with T_e ranging from 60 K to 200 K, n_e between 0.03 and 0.05 cm^{-3}and l between 4 pc and 90 pc fitted the data. Finally, if the angular size of the clouds is 2° then

models with T_e ranging from 150 K to 300 K, $n_e \sim 0.03$ cm^{-3}and l between 40 pc and 170 pc could explain the observations.

The range of possible physical parameters suggest that the line-forming regions may be associated with photo-dissociation regions. Although photo-dissociation regions are known to be widespread in the Galactic disk, carbon lines are detected only in about 30% of the observed positions. We attribute the paucity of the detections to (a) limitation of sensitivity, (b) lack of strong background radiation in some directions and (c) variation in the physical parameters of photo-dissociation regions. Further observations of low frequency carbon recombination lines with higher sensitivity are likely to yeild many more detections.

Acknowledgements

This work was done when NGK was associated with the Raman Research Institute, Bangalore and the Joint Astronomy Programme, Indian Institute of Science, Bangalore. We thank A. Santhosh Kumar for the installation and testing of the 8-line receiver and the operational staff at Gauribidanur for assistance with the long observations. We thank Anish Roshi for his generous help with the observations with the Ooty Radio Telescope and also for valuable discussions and thank K. S. Dwarakanath for help with the VLA observations. The National Radio Astronomy Observatory is a facility of the National Science Foundation operated under cooperative agreement by Associated Universities, Inc.

References

Altenhoff, W. J., Downes, D., Pauls, T., Schraml, J. 1979, *Astr. Astrophys.*, **35**, 23.

Anantharamaiah, K. R. 1985, *J. Astrophys. Astr.*, **6**, 177.

Anantharamaiah, K. R., Payne, H. E., Erickson, W. C. 1988, *Mon. Not. R. Astr. Soc.*, **235**, 151.

Anantharamaiah, K. R., Erickson, W. C., Payne, H. E., Kantharia, N. G. 1994, *Astrophys. J.*, **430**, 682.

Bania, T. M. 1977, *Astrophys. J.*, **216**, 381.

Bennett, C. L., Hinshaw, G. 1993, *In Back to the Galaxy*, Holt, S. S., Verter, F., editors, AIP, 257.

Blake, D. H., Crutcher, R. M., Watson, W. D. 1980, *Nature*, **287**, 707.

Burton, W. B. 1988, In *Galactic and Extragalactic Radio Astronomy*, Verschuur, G. I. & Kellerman, K. I., editors, Springer-Verlag, 295.

Deshpande, A. A., Shevgaonkar, R. K., Shastry, CH. V. 1989, *JIETE*, **35**, 342.

Downes, D., Wilson, T. L., Bieging, J., Wink, J. 1980, *Astr. Astrophys.*, **40**, 379.

Dwarakanath, K. S. 1989, *Ph.D. Thesis*, Indian Institute of Science, Bangalore.

Erickson, W. C., McConnell, D., Anantharamaiah, K. R. 1995, *Astrophys. J.*, **454**, 125.

Garwood, R. W., Dickey, J. M. 1989, *Astrophys. J.*, **338**, 341.

Golynkin, A. A., Konovalenko, A. A. 1991, *Sov. Astron. Lett.*, **17(1)**, 7.

Heiles, C. 1994, *Astrophys. J.*, **436**, 720.

Hollenbach, D. J., Takahashi, T., Tielens, A. G. G. M. 1991, *Astrophys. J.*, **377**, 192.

Kantharia, N. G., Anantharamaiah, K. R., Goss, W. M. 1998a, *Astrophys. J.*, **504**, 375.
Kantharia, N. G., Anantharamaiah, K. R., Payne, H. E. 1998b, *Astrophys. J.*, **506**, 758.
Konovalenko, A. A., Sodin, L. G. 1980, *Nature*, **283**, 360.
Konovalenko, A. A. 1984a, *Sov. Astron. Lett.*, **10(6)**, 384.
Lockman, F. J. 1976, *Astrophys. J.*, **209**, 429.
Lockman, F. J., Pisano, D. J., Howard G., J. 1996, *Astrophys. J. Lett.*, **472**, L173.
Mizutani, K. *et al.*, 1994, *Astrophy. J. Supple. Ser.*, **91**, 613.
Onello, J., Phillips, J. A., 1995, *Astrophys. J.*, **448**, 727.
Palmer, P., Zuckerman, B., Penfield, H., Liley, A. E., Mezger, P. G. 1967, *Nature*, **215**, 40.
Pankonin, V., Walmsley, C. M., Wilson, T. L., Thomasson, P. 1977, *Astr. Astrophys.*, **57**, 341.
Payne, H. E., Salpeter, E. E., Terzian, Y. 1984, *Astr. J.*, **89**, 668.
Payne, H. E., Anantharamaiah, K. R., Erickson, W. C. 1989, *Astrophys. J.*, **341**, 890.
Payne, H. E., Anantharamaiah, K. R., Erickson, W. C. 1994, *Astrophys. J.*, **430**, 690.
Pedlar, A., Davies, R. D., Hart, L., Shaver, P. A. 1978, *Mon. Not. R. Astr. Soc.*, **182**, 473.
Petuchowski, S. J., Bennett, C. L. 1993, *Astrophys. J.*, **405**, 591.
Reich, W., Fuerst, E., Reich, P., Reif, K. 1990, *Astr. Astrophys. Supple. Ser.*, **85**, 633.
Roelfsema, P. R., Goss, W. M., Wilson, T. L. 1987, *Astr. Astrophys.*, **174**, 232.
Roshi, A. D., Anantharamaiah, K. R. 1997, *Mon. Not. R. Astr. Soc.*,**292**, 63.
Roshi, A. D., Anantharamaiah, K. R. 2000, *Astrophys. J.*, **535**, 231.
Salem, M., Brocklehurst, M. 1979, *Astrophy. J Supple. Ser.*, **39**, 633.
Scoville, N.Z., Solomon, P.M. 1975, *Astrophys. J.*, **199**, L10.
Shaver, P. A. 1975, *Pramana*, **5**, 1.
Shibai *et al.*1991, *Astrophys. J.*, **374**, 522.
Smirnov, G. T., Kitaev, V. V., Sorochenko, R. L., Schegolev, A. F. 1996, In *Annual Session of Sci. Council of Astrocosmical Center of P.N.Lebedev Phys. Inst., Puschino 1995, Collection of Reports*, 3.
Sorochenko, R. L. 1996, *Astr. Astrophys. Trans.*, **11**, 199.
Subrahmanyan, R., Goss, W. M. 1996, *Mon: Not. R. Astr. Soc.*, **281**, 239.
Swarup, G., Sarma, N. V. G., Joshi, M. N., Kapahi, V. K., Bagri, D. S., Damle, S. H., Ananthakrishnan, S., Balasubramanian, V., Bahve, S. S., Sinha, R. P. 1971, *Nature*, **230**, 185.
Tielens, A. G. G. M., Hollenbach, D. J. 1985, *Astrophys. J.*, **291**, 722.
van Gorkom, J. H., Goss, W. M., Shaver, P. A., Schwarz, U. J., Harten, R. H. 1980, *Astr. Astrophys.*, **89**, 150.
Walmsley, C.M., Watson, W.D., 1982, *Astrophys. J.*, 260, 317.
Watson, W. D., Western, L. R., Christensen, R. B. 1980, *Astrophys. J.*, **240**, 959.